VIP Amorphous Materials Very Important Paper

DOI: 10.1002/anie.201404223

Bonding Nature of Local Structural Motifs in Amorphous GeTe**

Volker L. Deringer, Wei Zhang, Marck Lumeij, Stefan Maintz, Matthias Wuttig, Riccardo Mazzarello, and Richard Dronskowski**

Abstract: *Despite its simple chemical constitution and unparalleled technological importance, the phase-change material germanium telluride (GeTe) still poses fundamental questions. In particular, the bonding mechanisms in amorphous GeTe have remained elusive to date, owing to the lack of suitable bond-analysis tools. Herein, we introduce a bonding indicator for amorphous structures, dubbed "bond-weighted distribution function" (BWDF), and we apply this method to amorphous GeTe. The results underline a peculiar role of homopolar Ge–Ge bonds, which locally stabilize tetrahedral fragments but not the global network. This atom-resolved (i.e., chemical) perspective has implications for the stability of amorphous "zero bits" and thus for the technologically relevant resistance-drift phenomenon.*

Memory devices based on phase-change materials (PCMs)[1] encode digital data by exploiting an electronic contrast between two solid-state phases, typically an amorphous and a crystalline one, which can be rapidly switched back and forth. Among the most important ones is the apparently simple germanium telluride (GeTe): not only being a prototype PCM with diverse applications, it also forms the parent compound for a family of quasibinary alloys, such as $Ge_2Sb_2Te_5$, which are widely used in phase-change memories.[1] Until today, chemical bonding in crystalline PCMs along the GeTe-Sb_2Te_3 line has been thoroughly investigated.[2] For example, a bonding analysis of crystalline $GeSb_2Te_4$ revealed why the material forms a large number of intrinsic vacancies;[2a] these vacancies were then shown to play a crucial role for the peculiar disorder-induced metal–insulator transitions (MITs) in these PCMs.[2c] In contrast, amorphous PCMs are still under lively debate, even the simple binary GeTe.[3]

To gain atomistic insight into these important and complex amorphous phases, ab initio molecular-dynamics (MD) simulations have been firmly established;[4] indeed, results from current MD techniques compare favorably to experimental observables, such as Raman[4c] and XANES spectra.[4f] Beyond that, however, it is now crucial to understand the chemical-bonding nature of amorphous PCMs, as advocated by Xu et al.;[5] especially, a side-by-side comparison of crystalline and amorphous GeTe would be valuable but is yet missing. There is not only academic interest in these phases but also a very practical need: the atomistic origins of the resistance-drift phenomenon (structural changes in the amorphous phase over time) need to be understood, because this phenomenon hinders the development of multi-level storage;[6] in the long run, a chemical viewpoint may contribute decisive puzzle pieces. Furthermore, chemical-bonding indicators may even be utilized to design novel PCMs.[2b]

In fact, the electronic wavefunctions that are routinely obtained from the aforementioned simulations do already contain the precious bonding information, but this information is not directly accessible and must be extracted using suitable tools. Among them, the crystal orbital overlap population (COOP)[7] can reveal the nature of covalent interactions in solids: bonding (stabilizing) contributions to the electronic band structure are identified by positive orbital overlaps, whereas antibonding ones give negative COOPs. The subsequently developed crystal orbital Hamilton population (COHP)[8] builds on similar concepts and is the very method previously applied to crystalline $GeSb_2Te_4$;[2a] the difference between both techniques is the criterion chosen to gauge bonding interactions (orbital overlap in the COOP framework; energy contributions for COHP). To date, these analyses have been mostly restricted to small simulation cells and rather homogeneously packed structures, for simple technical reasons. Recently, we have shown how to extract similar information from numerically efficient plane-wave basis sets,[9,10] the workhorses of today's materials simulations, which can handle simulation cells on the order of hundreds of atoms. This enables a "projected COOP" (pCOOP) to be calculated from the plane-wave based density-functional theory output and, hence, analyze large systems—including models of amorphous PCMs from the aforementioned MD simulations.

Herein, we describe our first application of this method to an amorphous system: namely, to the amorphous phase of GeTe (a-GeTe). To make such analysis tractable and handle

[*] Dipl.-Chem. V. L. Deringer, Dr. M. Lumeij, Dipl.-Chem. S. Maintz, Prof. Dr. R. Dronskowski
Institute of Inorganic Chemistry
RWTH Aachen University
Landoltweg 1, 52056 Aachen (Germany)
E-mail: drons@HAL9000.ac.rwth-aachen.de
Dr. W. Zhang, Prof. Dr. R. Mazzarello
Institute for Theoretical Solid-State Physics
RWTH Aachen University
52074 Aachen (Germany)
E-mail: mazzarello@physik.rwth-aachen.de
Prof. Dr. M. Wuttig
Institute of Physics IA, RWTH Aachen University
52074 Aachen (Germany)
Prof. Dr. M. Wuttig, Prof. Dr. R. Mazzarello, Prof. Dr. R. Dronskowski
Jülich-Aachen Research Alliance (JARA-FIT and JARA-HPC), RWTH Aachen University, 52074 Aachen (Germany)

[**] We thank the Studienstiftung des deutschen Volkes for a scholarship (V.L.D.), the Deutsche Forschungsgemeinschaft for funding (SFB 917 "Nanoswitches"), and the IT center at RWTH Aachen University for CPU time.

Supporting information for this article is available on the WWW under http://dx.doi.org/10.1002/anie.201404223.

the structural complexity of a-GeTe, it will be necessary to introduce a novel distribution function that builds on atom-pair-wise indicators such as, in this case, the pCOOP.

We start by briefly reflecting on crystalline GeTe, for which bond-analytical curves are shown in Figure 1 a. The pCOOP analysis reveals strongly stabilizing contributions in the s and p valence bands; however, a filled but destabilizing area (starting at about 2 eV below the Fermi level ε_F) exists as well, as seen in related PCMs.[2a] A previous COHP analysis of GeTe already showed such an antibonding peak, which may be traced back to Ge 4s-Te 5p interactions.[12]

Moving on to a-GeTe, which we model using 216-atom cells (see Methods Section), its electronic DOS is shown in Figure 1 b, and the valence region may be divided into three parts (labeled "A" to "C"). Comparing the DOS of a-GeTe with that of crystalline GeTe, the closure of the gap between regions A and B is observed, as has been described for related PCMs.[4b] The pCOOP in Figure 1 b was obtained by averaging over all heteropolar (Ge–Te type) contacts up to 3.0 Å in the amorphous network. There is significant covalent bonding in region A, stemming mainly from the s orbitals, much less in the B set of bands. Region C exhibits an antibonding peak below ε_F that appears similar to what is seen in crystalline GeTe (Figure 1 a). Hence, the shape of the averaged pCOOP curve alone would suggest similarity to crystalline GeTe; this is not obvious as the atomic environments are different in the two phases. However, as will become apparent in the following, averaging over all bonds in the entire simulation cell will not suffice for a well-rounded picture. Furthermore, the homopolar Ge–Ge contacts, neglected so far, will be shown to play a central role in a-GeTe.

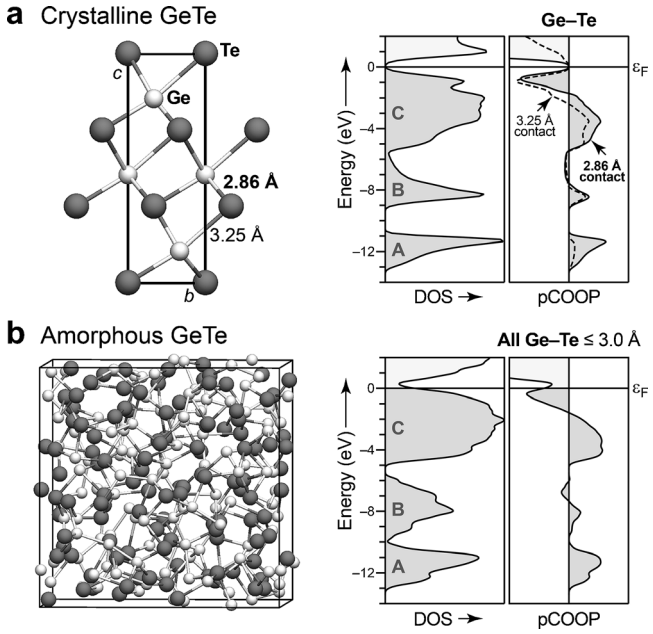

Figure 1. a) Structure of crystalline GeTe (from Ref. [11]), with "short" and "longer" contacts indicated. Densities of states (DOS) and projected crystal orbital overlap populations (pCOOP) are shown on the right. b) Snapshot from an MD simulation of a-GeTe and bonding analysis for this structural model. The pCOOP curve has been averaged over all Ge–Te contacts up to 3.0 Å in length.

While the shape of a COOP curve reveals the bonding character between any two atoms A and B, its integration up to ε_F yields a measure of the A–B bond strength.[7] We call the integrated COOP "bond population", B_{AB}, in the following [Eq. (1)].

$$B_{AB} = \int_{-\infty}^{\varepsilon_F} \mathrm{pCOOP}_{AB}(E)\,dE \qquad (1)$$

To improve the statistics, we now consider ten structural snapshots from the MD trajectory at 300 K, taken at intervals of 3 ps and subsequently fully relaxed; for each snapshot, a set of B_{AB} is obtained. Figure 2 a provides a scatterplot where all contacts up to 7 Å have been taken into account, including interatomic distances much longer than typical cutoffs used to define bonds in a-GeTe. The dataset comprises 51 640 individual contacts, an improvement by orders of magnitude upon previously possible COOP/COHP analyses.

Figure 2 a is comprehensive but contains a very high density of information. To ease understanding, the data would now be condensed into a radial distribution function (RDF). Herein, utilizing the pCOOP technique, we are able to extend the concept of the RDF to define a more generalized distribution function which also contains information about

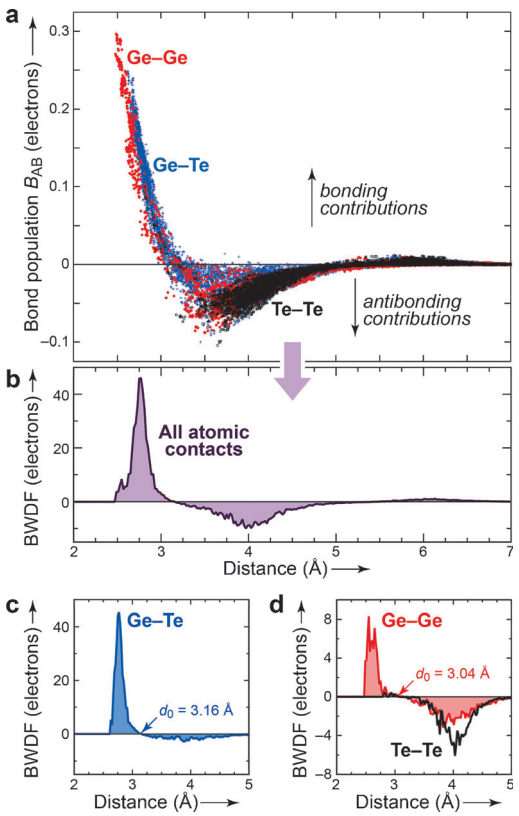

Figure 2. a) Scatterplot of bond populations in amorphous GeTe, collected over all atomic contacts up to 7 Å and over ten relaxed MD snapshots. b) Bond-weighted distribution function (BWDF) derived from the data points above and hence summed up over all simulation cells [cf. Eq. (2)]. c) Selective BWDF for heteropolar contacts, with the apparent cutoff d_0 indicated. d) Same but for either type of homopolar contacts. d_0 is given for Ge–Ge bonds but not for Te–Te because the Te–Te bonds show no noticeable stabilization.

the bonding character.[13] More precisely, we use the bond population B_{AB} to introduce a "bond-weighted distribution function" (BWDF) given by Equation (2).

$$\mathrm{BWDF} = \sum_{B>A} [\delta(r - |\mathbf{r}_{AB}|) \times B_{AB}] \quad (2)$$

The result is plotted in Figure 2b. Interestingly, doing so leads to a new definition of bond-length cutoff, namely, the radius d_0 at which the BWDF intersects the horizontal zero: before d_0, the atomic interactions are attractive while beyond they are repelling. For more detailed insight, we now constrain the species A/B in Equation (2) to either Ge/Ge, Ge/Te, or to Te/Te, which yields partial BWDF curves for homopolar and heteropolar contacts. The Ge–Te BWDF shown in Figure 2c falls to zero at $d_0 = 3.16$ Å, close to the cutoff value obtained by some of us before using a different criterion, the first minimum of the partial pair correlation function (PPCF).[4c] The previously invoked cutoff criterion may have some degree of arbitrariness (e.g., when the PPCFs do not exhibit a clear minimum after the first peak), whereas the new definition seems free of ambiguities in principle, given a reliable projection.[13] For Ge–Ge contacts (Figure 2d), d_0 equals 3.04 Å, again close to previously used values. The overall magnitude of the Ge–Ge BWDF is lower than that for the heteropolar contacts, which reflects the fact that most covalent bonds in a-GeTe are of Ge–Te type. Longer Ge–Ge contacts above 3.5 Å display significant repelling character (BWDF < 0), whereas this is not as pronounced for long Ge–Te contacts. Finally, all Te–Te contacts emerge as repelling, as expected. At distances above approximately 5 Å, the BWDF drops to zero, because covalent bonding is a short-range phenomenon that requires a non-vanishing degree of orbital overlap.

Ab initio models of amorphous GeTe obtained by fast quenching from the melt invariably contain a notable amount of tetrahedrally coordinated germanium atoms, a striking structural feature absent in the crystalline phase. These tetrahedral fragments rarely contain four Te ligands but at least one homopolar Ge–Ge bond,[4c] as sketched in Figure 3a. To understand the stability of these structural motifs, it is crucial to investigate the chemical nature of the contacts in more detail. To this end, we consider partial BWDFs, obtained by including only the bonds which belong to tetrahedral fragments, or those in defective octahedral GeX_4 configurations. To discriminate between both, we use the same order parameter as in Ref. [4a].

Interestingly, homopolar Ge–Ge contacts (Figure 3b) seem to have strongly different bonding nature, depending on whether they partake in tetrahedral or octahedral motifs. In tetrahedra, the BWDF exhibits a more significant bonding peak at short distances of approximately 2.6 Å; Ge–Ge bonds in tetrahedra seem chemically quite strong. For octahedral environments, on the other hand, Figure 3b does not suggest significant Ge–Ge bonding, because the positive BWDF region is counterbalanced by an antibonding one at longer distances. Turning to heteropolar bonds (which are more abundant and hence exhibit higher absolute BWDF values), the nature of Ge–Te contacts is rather independent of the local structure, and the two BWDF curves in Figure 3c are

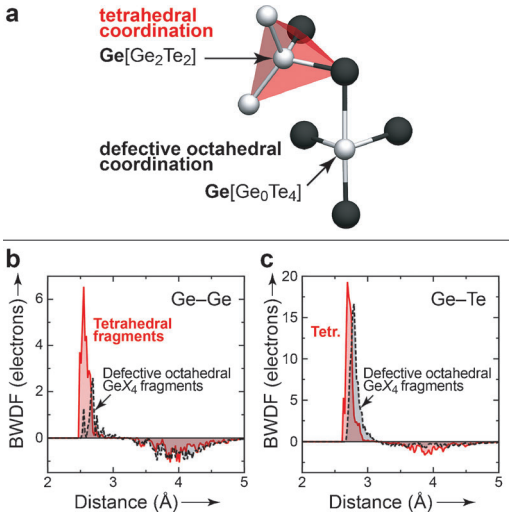

Figure 3. a) Structural fragment from the model shown in Figure 1a, drawn to emphasize the different coordination motifs found in the amorphous phase. b,c) BWDFs as before, but separated into homopolar (Ge–Ge) and heteropolar (Ge–Te) contacts, and also according to the coordination environments; see text.

quite similar. It may be concluded that homopolar bonds stabilize tetrahedral motifs in a-GeTe, but they do not significantly strengthen octahedral motifs. Accordingly, crystalline GeTe, composed entirely of distorted octahedra, does not show nearest-neighbor Ge–Ge interactions.

We have also collected pCOOP curves specifically for tetrahedral motifs in a-GeTe, aiming to verify the previously posed hypothesis that the tetrahedral units are strengthened by homopolar bonds.[4a,c] Figure 4 presents results for GeX_4 motifs, again separated into tetrahedral and defective octahedral sites. Since we want to probe the influence of Ge–Ge bonds on the stability of the two configurations, we start by looking at $GeTe_4$ fragments with no Ge–Ge contacts, and in the next step we consider mixed homo-/heteropolar environments. The pCOOP curve on the left of Figure 4 shows a pronounced instability for tetrahedral $GeTe_4$ motifs, that is, a major antibonding peak at ε_F. This agrees with the fact that pure $GeTe_4$ tetrahedra are rarely observed in ab initio models of a-GeTe. On the contrary, with one or two homopolar bonds present (middle and right panel in Figure 4), these antibonding interactions for tetrahedra decrease significantly. Homopolar contacts do seem to make tetrahedral motifs more favorable, if judging from the shape of the pCOOP curves alone. Note that the removal of antibonding interactions is a purely structural consequence and does not go back to a lowered electron count since the exchange of Te by Ge in the first coordination shell leaves the overall composition unchanged. In contrast, the influence of the bond type seems lower for octahedral motifs, as evidenced by the corresponding pCOOP curves (dashed black lines). We stress that Figure 4 provides information only about the relative stability of the local structural motifs, whereas the global stability of the amorphous network depends on longer range order, too.

In conclusion, we have developed new tools which afford an atom-resolved analysis of chemical bonding in amorphous structures. Our bond-weighted distribution function (BWDF)

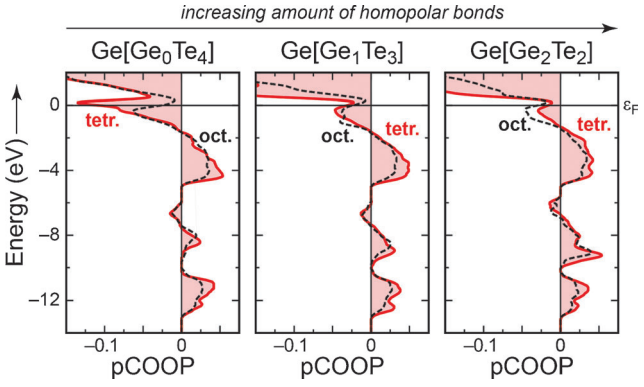

Figure 4. pCOOP analysis resolved according to GeX_4 motifs in one of the structural snapshots. pCOOPs (per bond) are averaged separately for tetrahedral and defective octahedral motifs.

combines the valuable bonding information with a geometrical tool, namely, the well-established radial distribution function. This analysis provides new evidence that in a-GeTe, tetrahedral fragments are indeed stabilized by homopolar bonds whereas defective octahedral environments are not. Open questions remain with regard to the global stability of the amorphous network as obtained by fast MD quenching. More specifically, it is not understood if the presence of a large amount of homopolar bonds and tetrahedral motifs results from the fast quenching times, and how these motifs evolve over time. This issue, which is closely linked to the resistance-drift phenomenon, will be the subject of future work.

Computational Methods

Amorphous GeTe was modeled by ab initio MD, using a novel Car-Parrinello-like scheme[14] as implemented in CP2K,[15] a generalized gradient approximation (GGA) potential,[16] and Goedecker-Teter-Hutter pseudopotentials.[17] The supercell contained 216 atoms, and its Brillouin zone was sampled at Γ. The timestep was 2 fs. The model was randomized at 3000 K and then gradually quenched to the melting temperature (1100 K) within 20 ps. After equilibrium at the melt (30 ps), the system was quenched to 300 K over 90 ps.

Ten snapshots from the trajectory were then fully relaxed (at 0 K) at the GGA level of density-functional theory (DFT),[16] using the projector augmented-wave method[18] as implemented in VASP.[19] Self-consistent wavefunctions were computed for the relaxed models and projected onto a local basis of Slater type orbitals; the thus obtained atomic-orbital coefficients were orthonormalized using Löwdin's approach.[10] The quality of the projection was measured by the charge spilling parameter[20] which in this case amounts to $S_O \approx 0.06$; this is appreciable given the complexity of the problem. In the future, individually optimized basis sets might be considered to reduce S_O further, which however is expected to make few changes to the concepts shown herein.

Received: April 11, 2014
Published online: July 17, 2014

Keywords: bond theory · crystal orbital overlap populations · molecular dynamics · phase-change materials · resistance drift

[1] For a Review, see: M. Wuttig, N. Yamada, *Nat. Mater.* **2007**, *6*, 824.
[2] a) M. Wuttig, D. Lüsebrink, D. Wamwangi, W. Wełnic, M. Gilleßen, R. Dronskowski, *Nat. Mater.* **2007**, *6*, 122; b) D. Lencer, M. Salinga, B. Grabowski, T. Hickel, J. Neugebauer, M. Wuttig, *Nat. Mater.* **2008**, *7*, 972; c) W. Zhang, A. Thiess, P. Zalden, R. Zeller, P. H. Dederichs, J.-Y. Raty, M. Wuttig, S. Blügel, R. Mazzarello, *Nat. Mater.* **2012**, *11*, 952.
[3] a) A. V. Kolobov, P. Fons, A. I. Frenkel, A. I. Ankudinov, J. Tominaga, T. Uruga, *Nat. Mater.* **2004**, *3*, 703; b) D. A. Baker, M. A. Paesler, G. Lucovsky, S. C. Agarwal, P. C. Taylor, *Phys. Rev. Lett.* **2006**, *96*, 255501; c) B. Huang, J. Robertson, *Phys. Rev. B* **2010**, *81*, 081204; d) A. V. Kolobov, M. Krbal, P. Fons, J. Tominaga, T. Uruga, *Nat. Chem.* **2011**, *3*, 311.
[4] a) S. Caravati, M. Bernasconi, T. D. Kühne, M. Krack, M. Parrinello, *Appl. Phys. Lett.* **2007**, *91*, 171906; b) J. Akola, R. O. Jones, *J. Phys. Condens. Matter* **2008**, *20*, 465103; c) R. Mazzarello, S. Caravati, S. Angioletti-Uberti, M. Bernasconi, M. Parrinello, *Phys. Rev. Lett.* **2010**, *104*, 085503; d) S. Caravati, D. Colleoni, R. Mazzarello, T. D. Kühne, M. Krack, M. Bernasconi, M. Parrinello, *J. Phys. Condens. Matter* **2011**, *23*, 265801; e) D. Loke, T. H. Lee, W. J. Wang, L. P. Shi, R. Zhao, Y. C. Yeo, T. C. Chong, S. R. Elliott, *Science* **2012**, *336*, 1566; f) M. Krbal, A. V. Kolobov, P. Fons, K. V. Mitrofanov, Y. Tamenori, J. Hegedüs, S. R. Elliott, J. Tominaga, *Appl. Phys. Lett.* **2013**, *102*, 111904.
[5] M. Xu, Y. Q. Cheng, H. W. Sheng, E. Ma, *Phys. Rev. Lett.* **2009**, *103*, 195502.
[6] a) D. Ielmini, A. L. Lacaita, D. Mantegazza, *IEEE Trans. Electron Devices* **2007**, *54*, 308; b) P. Fantini, S. Brazzelli, E. Cazzini, A. Mani, *Appl. Phys. Lett.* **2012**, *100*, 013505.
[7] T. Hughbanks, R. Hoffmann, *J. Am. Chem. Soc.* **1983**, *105*, 3528.
[8] R. Dronskowski, P. E. Blöchl, *J. Phys. Chem.* **1993**, *97*, 8617.
[9] V. L. Deringer, A. L. Tchougréeff, R. Dronskowski, *J. Phys. Chem. A* **2011**, *115*, 5461.
[10] S. Maintz, V. L. Deringer, A. L. Tchougréeff, R. Dronskowski, *J. Comput. Chem.* **2013**, *34*, 2557.
[11] V. L. Deringer, M. Lumeij, R. Dronskowski, *J. Phys. Chem. C* **2012**, *116*, 15801.
[12] U. W. Waghmare, N. A. Spaldin, H. C. Kandpal, R. Seshadri, *Phys. Rev. B* **2003**, *67*, 125111.
[13] We use overlap, rather than Hamilton populations, partly because we have previously seen the pCOOP to be more robust with regard to projection quality, given the presently available basis sets: V. L. Deringer, R. Dronskowski, *Chem. Sci.* **2014**, *5*, 894. In principle, nonetheless, the BWDF [Eq. (2)] may be defined using any suitable numerical quantity that gives indication of pairwise interactions. This may, however, influence the shape of the curves and the zero intersect d_0, depending on the criterion chosen.
[14] T. D. Kühne, M. Krack, F. R. Mohamed, M. Parrinello, *Phys. Rev. Lett.* **2007**, *98*, 066401.
[15] J. van de Vondele, M. Krack, F. Mohamed, M. Parrinello, T. Chassaing, J. Hutter, *Comput. Phys. Commun.* **2005**, *167*, 103.
[16] J. P. Perdew, K. Burke, M. Ernzerhof, *Phys. Rev. Lett.* **1996**, *77*, 3865.
[17] S. Goedecker, M. Teter, J. Hutter, *Phys. Rev. B* **1996**, *54*, 1703.
[18] P. E. Blöchl, *Phys. Rev. B* **1994**, *50*, 17953.
[19] a) G. Kresse, J. Hafner, *Phys. Rev. B* **1993**, *47*, 558; b) G. Kresse, J. Furthmüller, *Phys. Rev. B* **1996**, *54*, 11169; c) G. Kresse, D. Joubert, *Phys. Rev. B* **1999**, *59*, 1758.
[20] D. Sánchez-Portal, E. Artacho, J. M. Soler, *Solid State Commun.* **1995**, *95*, 685.